

The Dependence of Plasma Ionization Equilibrium on Electron and Radiation Temperatures

Julia L. Tucker

Brighton High School
Rochester, NY

Advisor: Dr. Reuben Epstein

February 26, 2013

Laboratory for Laser Energetics
University of Rochester
Rochester, NY

Abstract

The atomic-physics radiation-transport simulation program PrismSpect [Prism Computational Sciences, Inc., Madison; WI., J. J. MacFarlane, I. E. Golovkin, P. Wang, P. R. Woodruff, and N. A. Pereyra, *High Energy Density Phys.* **3**, 181 (2007)] has been used to calculate the ionization state of germanium and silicon additives under conditions expected in plastic ablator shells imploded by indirect drive [J. D. Lindl, *et al.*, *Phys. Plasmas* **11**, 339 (2004)] on the National Ignition Facility (NIF) [G. H. Miller, *et al.*, *Opt. Eng.* **43**, 2841 (2004)]. The ionization equilibrium of the shell dopants may be altered by external radiation emitted by the hohlraum wall during the implosion and by the compressed deuterium-tritium (DT) core during ignition [S. P. Regan, R. Epstein, *et al.* *Phys. Plasmas* **19**, 056307 (2012)]. PrismSpect allows the user to vary the plasma conditions, the plasma composition, and the external radiation temperature and to view the spectra, mean charge, and fractional ionization species populations produced. A radiation-modified version of the Saha equation has been numerically programmed in Matlab [MATLAB version 7.10.0, Natick, Massachusetts: The MathWorks Inc., 2010] to provide an additional view of the effects of radiation on the ionization state of the shell additives. The PrismSpect and radiation-modified Saha results show that a radiation temperature around 300 eV, which is characteristic of the radiation emitted by a hohlraum, does not noticeably affect the ionization for electron temperatures above about 500 eV, and radiation emitted by a DT core does not substantially affect the ionization equilibria.

Introduction

Fusion occurs when intense heat and pressure are applied to an appropriately designed spherical target, causing the target to implode. When a target implodes, the outer portion of the target gives off energy and compresses the rest of the target inward. The compressed components of the target turn into plasma, fuse, and emit energy. This heat and pressure is applied through the use of many laser beams, all hitting the target at once from different angles.¹

There are two ways to implode a target: through direct-drive fusion and indirect-drive fusion. In direct-drive fusion, the lasers come in from all directions and directly hit the target to cause it to implode.² In indirect-drive fusion, the target is placed in a hollow gold cylinder called a hohlraum. The lasers enter through the open ends of the hohlraum and hit the inner walls of the cylinder. X rays are then radiated from the walls and heat the target. The targets are composed of a fuel mixture of deuterium and tritium (DT) gases, which are isotopes of hydrogen. The outermost layer of the gases is frozen, making the target “cryogenic”, and is covered in a plastic shell.

Target shells used in both direct-drive and indirect-drive fusion experiments can be doped with a concentration by atom of up to about 1% silicon (Si) or germanium (Ge).³ A Si shell dopant heats the shell by absorbing radiation from the ablation region, or the region that first gives off energy after being heated by the lasers. This radiation expands the shell and decreases its density, making the target more stable during implosion. Both Si and Ge dopants help protect the DT ice layer from being preheated by x rays emitted by the hohlraum in indirect-drive experiments on the National Ignition Facility (NIF).⁴ Hohlraums emit x-ray radiation with a radiation temperature of up to 300 eV, which could affect the ionization of the dopants when they mix with the hot, compressed DT core. The imploded core also emits radiation,

approximated here by a modified Planck spectrum with characteristic spectral and radiation temperatures. Radiation from either a hohlraum or a DT core can alter the ionization equilibrium of the shell dopant, which would then affect various properties of the plasma, such as its thermal conductivity, equation of state, and optical properties.

1. PrismSpect

PrismSpect⁵ is an atomic-physics radiation-transport program used to simulate the atomic level populations and radiative emission of plasmas over a range of controllable parameters, including temperature, density, and the radiation environment. After all the necessary information, such as target composition and size, has been entered, the program produces the resulting spectra, ionization, and line intensities. These results show the effect of radiation on the ionization. The overall mean charge, the electron density, the mean charge of each element in the plasma, and the ionization species fractions of each element are obtained. PrismSpect calculations are based on a detailed accounting of atomic states, allowing the user to choose which atomic states and configuration detail levels should be included. The calculations take into account a multitude of electron-electron and electron-photon interactions, such as collisional ionization, collisional (or 3 body) recombination, excitation, decay, photoionization, radiative recombination, stimulated emission, spontaneous emission, photoexcitation, and dielectronic recombination.^{6,7} The program includes the option to expose the target to an external radiation source.

PrismSpect also allows the user to choose among a few basic plasma configurations. Targets can be zero-width, planar, or spherical, and external radiation, if included, can be one-sided or two-sided. Electron temperature and mass density can be specified. The ability to control the

composition and configuration of the plasma and the atomic model through the user interface (Fig. 1) provides for a wide variety of simulations. The atomic kinetic model can be local thermodynamic equilibrium (LTE), or non-LTE. In LTE, all temperatures, such as radiation temperature and electron temperature, are equal, and conversely, non-LTE encompasses everything else. When a target is in non-LTE, where it is not exposed to any external radiation, and where all the self-emitted radiation escapes freely, the target is in collisional-radiative equilibrium (CRE).

2. Plasma Properties

When a target is in non-LTE and exposed to external radiation, the ionization equilibrium of the shell dopant generally differs from when it is in LTE. Mean charge is the best single-parameter representation of the ionization state. It takes into account all of the various fractional ionization species. When the radiation temperature equals the electron temperature of the plasma, thermal equilibrium is restored. LTE conditions prevail, and the mean charge and fractional ionization species populations of the non-LTE target exposed to radiation become equal to those of an LTE target, as seen in PrismSpect results plotted in Fig. 2.

Optical depth, τ_ν , is a measure of the opacity of an object to light of frequency ν propagating along a given path. The intensity of light is diminished as it passes through an object along this path by the factor of $e^{-\tau_\nu}$. For a uniform sphere of radius R , the optical depth can be expressed as the product of the mass density, ρ , target radius, R , and the mass-absorption coefficient, μ_ν , $\tau_\nu = \rho R \mu_\nu$. As an object increases in mass density or radius, it becomes more optically thick and reabsorbs more self-emitted radiation, and this causes LTE conditions to be restored. As the

matter becomes more in equilibrium with its own radiation, its emission spectrum more closely resembles a Planck spectrum, as given by Planck's Law,

$$B_\nu(T) = \frac{2h\nu^3}{c^2} \frac{1}{e^{h\nu/kT} - 1}, \quad (1)$$

where $B_\nu(T)$ is the emitted specific intensity, h is Planck's constant, ν is the photon frequency, c is the speed of light, k is Boltzmann's constant, and T is the plasma temperature.⁶ The graphs in Fig. 3 show emission spectra in units of specific intensity, ergs per cm² per steradian per second per electron volt, for spherical targets at a temperature $T=100$ eV and at two areal densities, $\rho R = 0.001$ g/cm² and 0.1 g/cm². The blue line in each is the emission spectrum of the plasma, and the red line shows the Planck spectrum at $T=100$ eV. At the higher density, the target is optically thick over nearly the entire spectrum. This produces an LTE radiative equilibrium where the specific intensity of the target emission (blue curve) is equal to the Planck spectrum (red curve) given by Eq. (1).

3. Hohlraum Radiation

3.1 Modified Saha Equation

The Saha equation⁸ gives the ratio of the densities of two successive ionization state populations, n_1 and n_2 , in a plasma in LTE and is dependent on electron temperature, T_e , the electron density, n_e , and the ionization energy, χ . It is

$$\left(\frac{n_2}{n_1}\right)_{LTE} = \frac{1}{4\pi^{3/2} (n_e a_0^3)} \frac{g_2}{g_1} \left(\frac{kT_e}{\chi_H}\right)^{3/2} e^{-\chi/kT_e}, \quad (2)$$

where a_0 is the Bohr radius, g_1 and g_2 are the statistical weights of the two successive ionization states, and χ_H is the hydrogen ground-state ionization energy. The Saha equation was modified in the following way to include the non-LTE effects of photoionization and stimulated radiative recombination by external radiation.⁹

In steady state, the non-LTE ionization equilibrium of two ionization species occurs when the total ionization and recombination rates are in balance. This can be expressed as

$$n_1 [C_{12}(T_e, n_e) + R_{12}(T_e, T_R)] = n_2 [C_{21}(T_e, n_e) + R_{21}(T_e, T_R, n_e) + A_{21}(T_e, n_e)], \quad (3)$$

where $C_{12}(T_e, n_e)$ and $C_{21}(T_e, n_e)$ are the electron-collisional ionization and recombination rates, respectively, $R_{12}(T_e, T_R)$ and $R_{21}(T_e, T_R, n_e)$ are the photoionization and stimulated recombination rates, and $A_{21}(T_e, n_e)$ is the radiative recombination rate. Photoionization and stimulated recombination are driven by the ambient radiation field, which is assumed to be the Planck spectrum at a radiation temperature T_R given by Eq. (1). The collisional ionization and recombination processes are detailed-balance inverses of each other, so, in the absence of all radiative processes, and in steady state, they will produce the same LTE population ratio given by the Saha equation Eq. (2),

$$\left(\frac{n_2}{n_1}\right)_{LTE} = \left(\frac{C_{12}(T_e, n_e)}{C_{21}(T_e, n_e)}\right). \quad (4)$$

Using this expression, the non-LTE (NLTE) radiative equilibrium expression, Eq. (3), can be written as a correction to the LTE Saha result as,

$$\frac{(n_2/n_1)_{NLTE}}{(n_2/n_1)_{LTE}} = \frac{1 + R_{12}(T_e, T_R)/C_{12}(T_e, n_e)}{1 + [R_{21}(T_e, T_R, n_e) + A_{21}(T_e, n_e)]/C_{21}(T_e, n_e)}. \quad (5)$$

This two-species model neglects excited states and ionization species, other than the two considered, and autoionization and dielectronic recombination¹⁰ are neglected. Consequently, it

is not an approximation that can be relied on for quantitative calculations. It is useful for identifying ranges of conditions where radiation can be an important ionization effect, and it can be corroborated at specific temperatures and densities with PrismSpect⁵, which does not make these approximations.

The semi-classical collisional ionization rate is given by

$$C_{12}(T_e, n_e) = n_e 8a_0^2 \sqrt{\frac{2\pi\chi_H^4}{m_e (kT_e)^3}} \left[\frac{kT_e}{\chi} e^{-\chi/kT_e} - E_i\left(\frac{kT_e}{\chi}\right) \right], \quad (6)$$

where $E_i\left(\frac{kT_e}{\chi}\right)$ is the exponential integral $E_i(x) = \int_x^\infty e^{-t} \frac{dt}{t}$, and m_e is the electron mass. The collisional recombination rate $C_{21}(T_e, n_e)$ is obtained from Eqs. (2), (4), and (6). The radiative transition rates can be written as photon-frequency integrals over the ambient isotropic radiation specific intensity $I(\nu)$ and the corresponding frequency-dependent Einstein coefficients:^{7,8,10}

$A_{21}(\nu)$ for spontaneous emission, $B_{21}(\nu)$ for stimulated emission, and $B_{12}(\nu)$ for photoionization,

$$A_{12}(T_e, n_e) = \int_0^\infty A_{12}(\nu) d\nu, \quad (7)$$

$$R_{12}(T_e, n_e) = \int_0^\infty B_{12}(\nu) I(\nu) d\nu, \quad (8)$$

and

$$R_{21}(T_e, n_e) = \int_0^\infty B_{21}(\nu) I(\nu) d\nu. \quad (9)$$

Under LTE conditions, where $T_R = T_e$, so that $I(\nu) = B_\nu(T_e)$ and the species populations assume their LTE values, the Einstein coefficients must be consistent with the radiative detailed balance between photoionization and its reverse processes, spontaneous and stimulated radiative recombination. This condition is expressed as¹⁰

$$n_1^{LTE} B_{12}(\nu) B_\nu(T_e) = n_2^{LTE} [A_{21}(\nu) + B_{21}(\nu) B_\nu(T_e)] . \quad (10)$$

With this expression and Eq. (1), all three Einstein coefficients can be obtained from one. We choose to write the photoionization Einstein coefficient as

$$\frac{h\nu}{4\pi} B_{12}(\nu) = \frac{64\pi}{3\sqrt{3}} \alpha a_0^2 \frac{p}{z^2} \left(\frac{\chi}{h\nu} \right)^3 \quad (11)$$

in terms of the Kramers photoionization cross section,

$$\sigma_K(\nu) = \begin{cases} \frac{64\pi}{3\sqrt{3}} \alpha a_0^2 \frac{p}{z^2} \left(\frac{\chi}{h\nu} \right)^3 ; h\nu \geq \chi \\ 0 ; h\nu < \chi \end{cases} , \quad (12)$$

where $\alpha \cong 1/137$ is the fine-structure constant.⁸ The stimulated recombination emission coefficient

$$\frac{\chi}{4\pi} B_{21}(\nu) = \frac{64\pi}{3\sqrt{3}} \alpha a_0^2 \frac{p}{z^2} \left(\frac{\chi}{h\nu} \right)^4 \left(\frac{n_1}{n_2} \right)_{LTE} e^{-h\nu/kT_e} \quad (13)$$

and the spontaneous radiative recombination emission coefficient

$$\frac{c^2}{8\pi} A_{21}(\nu) = \frac{64\pi}{3\sqrt{3}} \alpha a_0^2 \frac{p}{z^2} \frac{\chi^3}{h^3 \nu} \left(\frac{n_1}{n_2} \right)_{LTE} e^{-h\nu/kT_e} \quad (14)$$

are identified using Eqs. (1), (10), and (11). Note that the expressions in Eqs. (13) and (14) are zero for $h\nu < \chi$, following Eq. (12). Consequently, the integration limits in Eqs. (7)-(9) become $\nu = \chi/h$ and $\nu \geq 0$.

Using Eqs. (1), (6)-(9), (11), (13), and (14), Eq. (5) can be evaluated, simplified, and expressed in the form

$$\frac{(n_2 / n_1)_{NLTE}}{(n_2 / n_1)_{LTE}} = \frac{1 + F(T_e, n_e) \int_{\frac{\chi}{h}}^{\infty} \frac{dv}{v} \frac{1}{(e^{\frac{hv}{kT_R}} - 1)}}{1 + F(T_e, n_e) \int_{\frac{\chi}{h}}^{\infty} \frac{dv}{v} \frac{e^{\frac{hv(\frac{1}{kT_R} - \frac{1}{kT_e})}}}{(e^{\frac{hv}{kT_R}} - 1)}}, \quad (15)$$

where

$$F(T_e, n_e) = \frac{\frac{64\pi}{3} \sqrt{\frac{\pi}{3}} \left(\frac{kT_e}{\chi}\right)^{3/2} \left(\frac{\chi}{ch}\right)^3 \frac{z}{n_e p^2}}{\frac{kT_e}{\chi} e^{-\chi/kT_e} - E_i \left(\frac{kT_e}{\chi}\right)}. \quad (16)$$

In the modified equation, the mean charge, z , and the principal quantum number, p , are variables that affect the ratio, in addition to the radiation temperature, T_R . The modified Saha equation continues to show a strong dependence on electron temperature and electron density and includes a radiative ionization and stimulated recombination correction factor applied to a collisional ionization and recombination ratio. The correction includes the function $F(T_e, n_e)$ and integrals over the Planck spectrum and absorption cross-section. The CRE value of n_2/n_1 is obtained for $T_R = 0$. When $T_R = T_e$, LTE conditions are restored, as confirmed by the PrismSpect results, and the radiation-modified Saha ratio given by Eq. (15) is equal to one. The T_R value that doubles the $T_R = 0$ value of the ratio given by Eq. (15) is taken somewhat arbitrarily as corresponding to the level of radiation required to significantly affect the ionization equilibrium. Doubling this ratio of successive species populations raises the average charge of that element, z_{avg} , by less than half a unit of charge. This is easily seen for T_e, n_e conditions where $n_1 = n_2$ at $T_R = 0$, for example, where $z_{avg} = (z_1 + z_2)/2$. Raising T_R from zero enough to double n_2/n_1

raises n_2 and lowers n_1 , bringing n_2 closer to, but not beyond its peak value, where $z_{avg} \leq z_2$.

Since $z_2 = z_1 + 1$, the change from $z_{avg} = (z_1 + z_2) / 2$ to $z_{avg} \leq z_2$ amounts to a change

$$\Delta z_{avg} \leq 1/2.$$

3.2 Analytical Results

A program was created in MATLAB¹¹ to evaluate the Saha equation correction given by Eq. (15). Fig. 4 shows results from this program. The graphs represent temperature space as a $T_e - T_R$ plane. To indicate the areas of significant radiation effects for Si and Ge, each graph has a red curve that shows where the Saha correction ratio doubles the Saha population ratio given by Eq. (2). The blue shaded area below the curve represents a radiation effect that is too small to be significant. The pink shaded area above the red curve represents where the radiation temperature will alter the ionization equilibrium significantly. The change from insignificant to significant radiation is simply a matter of our use of the doubled population ratio as a criterion to define where the effects of the radiation have become significant. Actually, the radiation effects change gradually as T_R increases continuously in moving from below to above this curve. Using this criterion, then, Fig. 4 shows that a hohlraum radiation temperature of around 300 eV does not significantly change the ionization equilibrium for electron temperatures above about 500 eV.

3.3 PrismSpect Results

PrismSpect was used to calculate mean charges of Si and Ge dopants for a range of radiation temperatures at various electron temperatures (Fig. 5). One can see that the mean charge of each dopant is quite static for a relatively high electron temperature of 2000 eV, but when the electron

temperature is lowered to 500 eV, the mean charge changes more noticeably at higher T_R . For both electron temperatures, the range of radiation temperatures characteristic of hohlraum interiors, up to 300 eV, does not produce a significant photoionization effect on the mean charge ($\Delta z \leq 1/2$), which is consistent with the conclusion drawn from the modified Saha results in Fig. 4. For the lower electron temperature, the radiation temperature must be at least ~ 400 eV to increase the mean charge by one charge unit, which can be considered significant, and the radiation temperature must be above the range of values shown in these graphs to have a significant effect at higher electron temperatures.

4. OMEGA Implosion Radiation

As a target implodes, its core radiates, and the radiation absorbed by the shell dopant may affect the ionization of the shell dopant. A simulation⁹ of the direct-drive OMEGA shot #62205 using the one-dimensional hydrodynamics code LILAC¹² was used to calculate the emission of the core of a representative cryogenic implosion. This emission takes place 4.2 ns after the onset of the laser pulse on the target, which has imploded at this time to a DT sphere with a radius of 25 microns, an areal density of 75 mg/cm^2 , and an electron temperature of 2000 eV. The emission spectrum is plotted as the “Simulated Intensity” in Fig. 6, and can be used as external radiation input in PrismSpect in order to view the effects of core radiation on the dopant. This external radiation can be represented in PrismSpect most generally by a two-temperature specific intensity of the form

$$I_\nu = \left(\frac{T_R}{T_S} \right)^4 B_\nu(T_S) . \quad (17)$$

This uses the radiation temperature T_R and a separate spectral temperature T_S to give a specific intensity with the spectral form of a Planck spectrum of temperature T_S and a spectral integral equal to that of a Planck spectrum of temperature T_R . A spectral temperature of 330 eV and a radiation temperature of 600 eV created a (purple) curve that fit the DT emission best. The Planck spectrum and its two-temperature generalization provide a well-understood and convenient parameterized representation of spectral intensity in studying the effects of externally applied radiation. The correct T_R and T_S were found by minimizing the spectral integral of the square of the difference between the simulated spectrum and the spectrum created using Eq. (17). This created the curve that most closely followed the simulated spectrum for photon energies around its peak intensity.

At low photon energy, the emission spectrum of the DT core in Fig. 6 follows a Planck spectrum of temperature equal to the core temperature $T = 2000$ eV, represented by the blue curve, as is expected, since the core is optically thick at the lowest photon energies. At higher photon energy, the emission spectrum, represented by the green curve, could be modeled by the equation

$$I_\nu = Ae^{-h\nu/kT} \quad , \quad (18)$$

with an upgraded version of PrismSpect. In Eq. (18), the intensity depends on a constant, A, the photon energy, ν , and the temperature, T. The green curve shows that this spectrum for $A = 4 \times 10^{19}$ and the same core temperature $T = 2000$ eV fits the DT emission better for high photon energies than the modified Planck spectrum presented by Eq. (17).

The radiation temperature of 600 eV, with a corresponding spectral temperature of 330 eV, was tested in PrismSpect to see how core radiation at these temperatures affect the mean charge.

Figure 7 shows the dependence of Si mean charge on electron temperature for three mass densities. It is clear in Figure 7 that the core radiation has a stronger effect on the mean charge for the lowest mass density. As the mass density increases, the mean charge of an irradiated plasma becomes almost identical to that of a plasma that is not exposed to radiation for the entire range of electron temperatures shown. This can be explained by the fact that, as density increases, ionization by electron collisions becomes more frequent than photoionization caused by radiation, thus reducing the effect of external radiation on the ionization. The core radiation, therefore, is unlikely to significantly alter the ionization of the plasma.

5. Conclusion

The program PrismSpect was used to simulate the effects of external radiation emitted by a hohlraum and a target core on the ionization equilibria of Si and Ge dopants. A program in MATLAB was also used to view the effects of radiation via a modified Saha equation that takes radiation temperature into account. Though both hohlraum radiation and core radiation have the potential to alter the ionization equilibrium of shell dopants, neither were found to change the equilibrium a significant amount under conditions of interest.

References:

1. Lois H. Gresh, Robert L. McCrory, and John M. Soures, *Inertial Confinement Fusion: An Introduction*, Laboratory for Laser Energetics: Rochester, NY, 2009.
2. J. D. Lindl, *et al.*, Phys. Plasmas **11**, 339 (2004).
3. S. P. Regan, R. Epstein, *et al.* Phys. Plasmas **19**, 056307 (2012).
4. G. H. Miller, *et al.*, Opt. Eng. **43**, 2841 (2004).
5. Prism Computational Sciences, Inc., Madison, WI.; J. J. MacFarlane, I. E. Golovkin, P. Wang, P. R. Woodruff, and N. A. Pereyra, High Energy Density Phys. **3**, 181 (2007).
6. L. Motz and A. Duveen, *Essentials of Physics* (Wadsworth, New York, 1967).
7. Y. B. Zel'dovich, Y. P. Raizer, W. D. Hayes, and R. F. Probstein, *Physics of Shock Waves and High-Temperature Hydrodynamic Phenomena* (Academic Press, New York, 1966) Vol. I.
8. G. C. Pomraning, *The Equations of Radiation Hydrodynamics* (Pergamon Press, New York, 1973).
9. R. Epstein, LLE, private communications (2012).
10. D. Salzman and A. Krumbein, J. Appl. Phys. **49**, 3229 (1978).
11. MATLAB version 7.10.0, Natick, Massachusetts: The MathWorks Inc., 2010.
12. J. A. Delettrez, R. Epstein, M. C. Richardson, P. A. Jaanimagi, and B. L. Henke, Phys. Rev. A **36**, 3926 (1987).

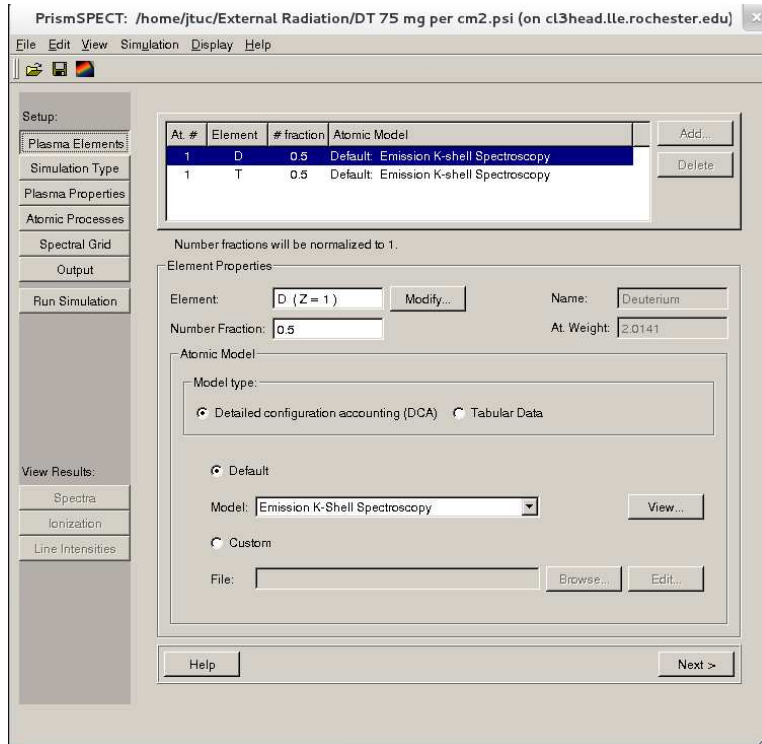


Figure 1: A screen-shot of the PrismSpect⁵ user interface shows the elemental composition of the plasma and lists further categories for specifying further conditions in the tabs on the left hand side.

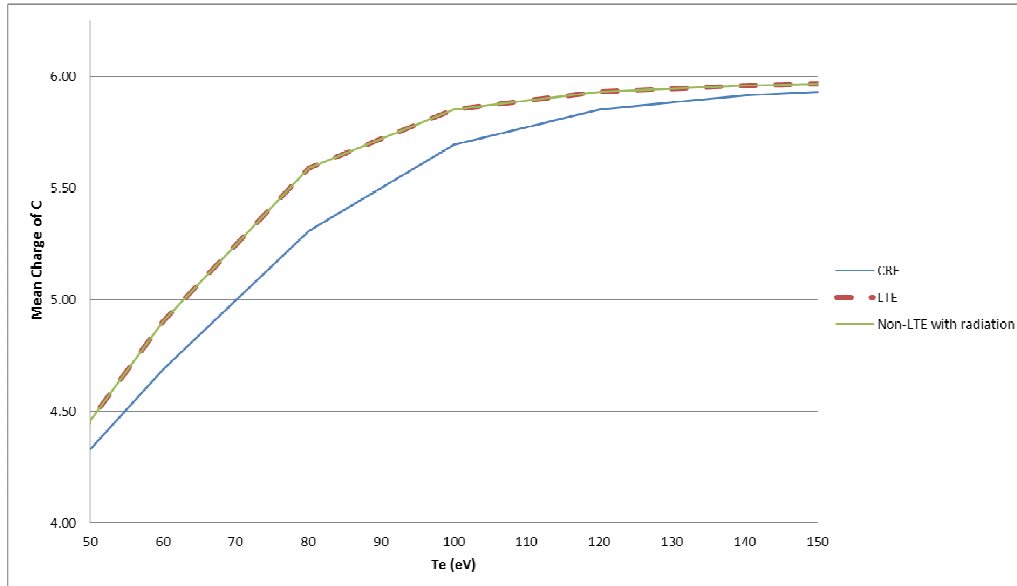
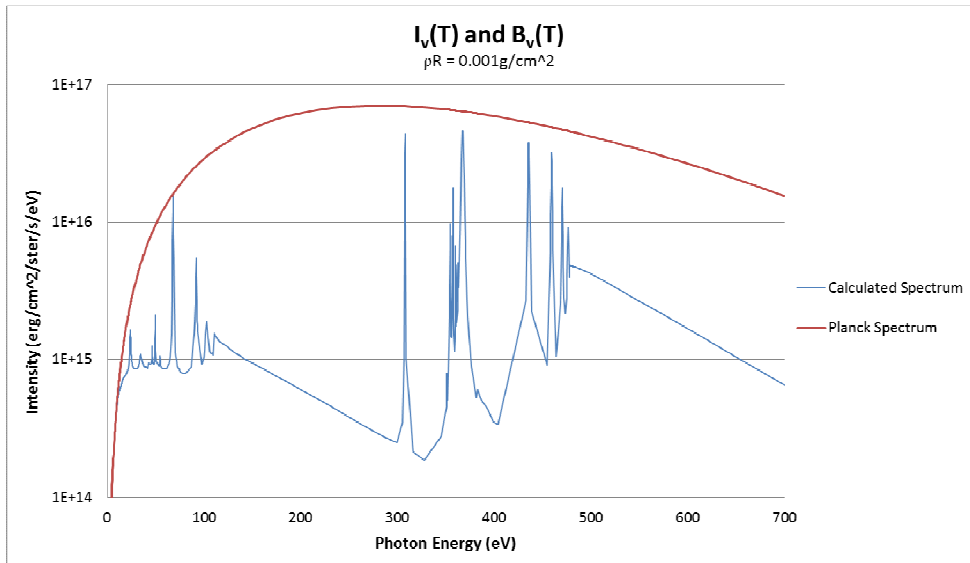
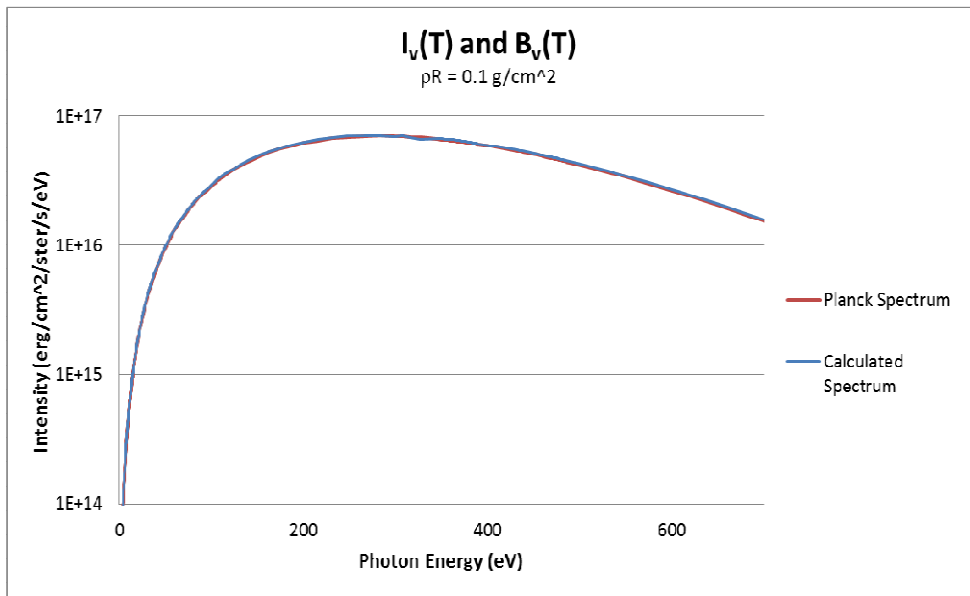


Figure 2: The effect of external radiation on the mean charge of carbon under target conditions in non-LTE with an electron density of $2.93 \times 10^{21} \text{ cm}^{-3}$. When radiation is applied that is the same temperature as the plasma temperature, the non-LTE curve exactly follows the LTE curve.



(a)



(b)

Figure 3: These two graphs show the emission spectra for a homogenous carbon sphere at a temperature of 100 eV. Graph (a) is for a target with an areal density of 0.001 g/cm^2 , while graph (b) has an areal density of 0.1 g/cm^2 . In graph (b), the two curves coincide completely so that only one may be visible.

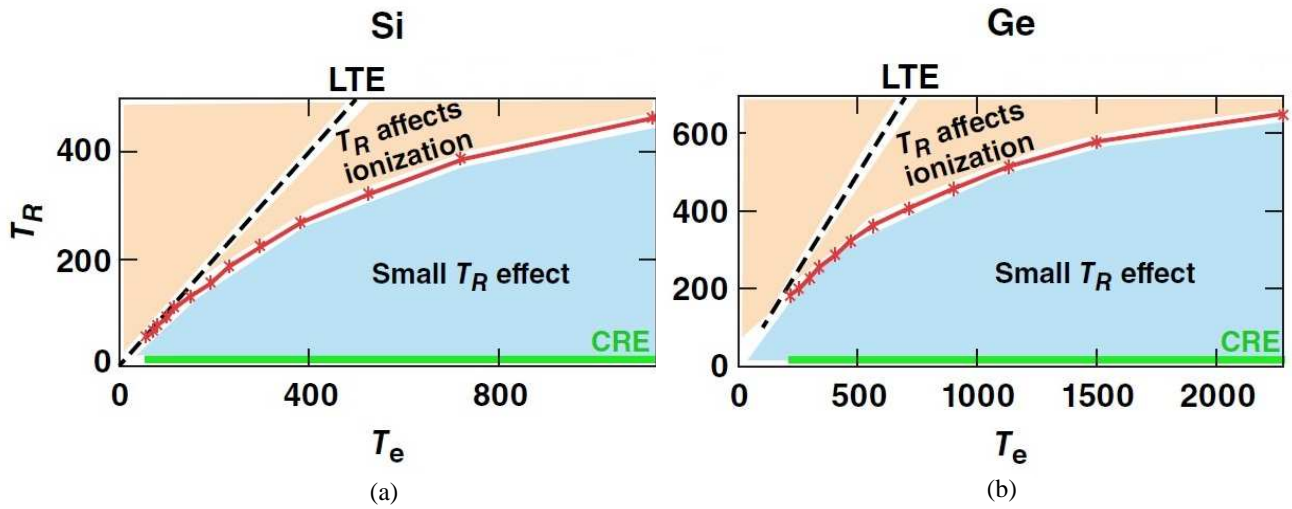


Figure 4: Regions where radiation either does or does not have a significant effect on the ionization state of a plasma for varying T_R and T_e . Plot (a) is for a Si plasma with an electron density of $1.3 \times 10^{23} \text{ cm}^{-3}$, and plot (b) is for a Ge plasma with an electron density of $1.2 \times 10^{23} \text{ cm}^{-3}$. The black line represents LTE conditions ($T_R = T_e$), the green line represents CRE conditions ($T_R = 0$), and the red curve represents where the Saha correction factor given by Eq. (15) doubles the ionization species population ratio given by the Saha equation, Eq. (2).

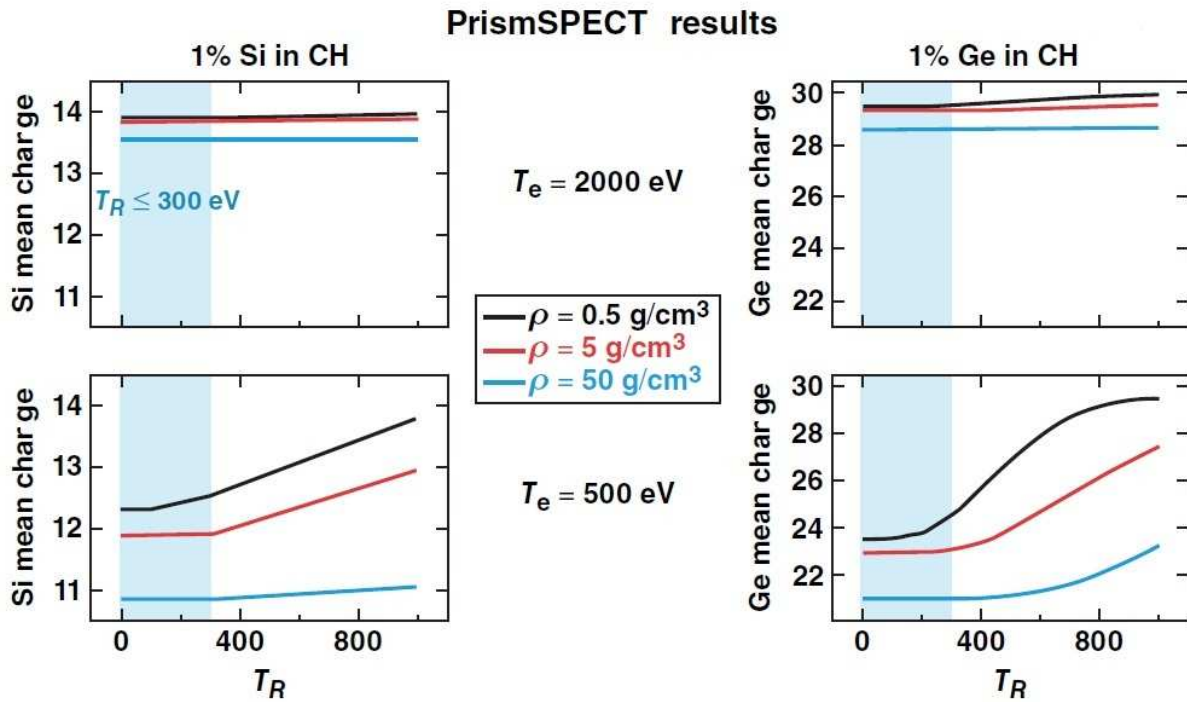


Figure 5: Dependence of the mean charge on radiation temperature for CH plasmas with a 1% Si or Ge dopant. The top set have an electron temperature of 2000 eV, and the lower set have an electron temperature of 500 eV. The different colored lines represent different mass densities.

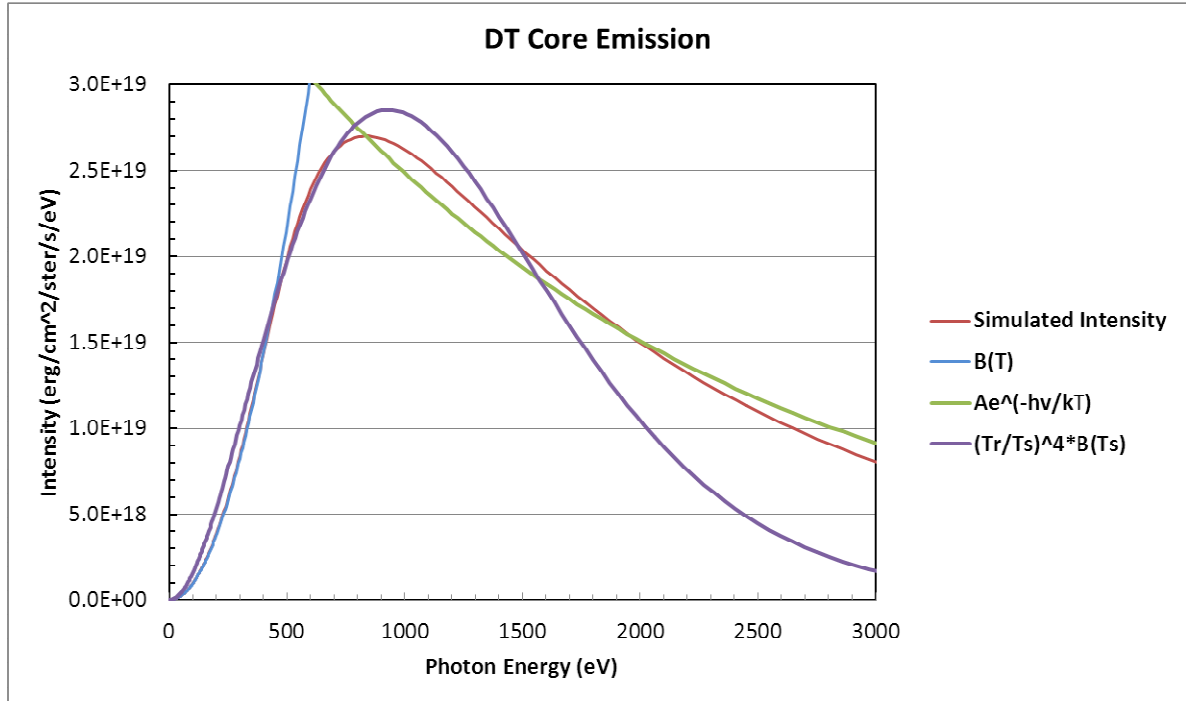


Figure 6: The red curve in this graph shows the emission of a DT core with mass areal density of 75 mg/cm^2 and core temperature $T = 2000 \text{ eV}$ at 4.2 ns into the implosion. The purple curve shows this spectrum as modeled by Eq. (17) with $T_S = 330 \text{ eV}$ and $T_R = 600 \text{ eV}$ and used as input to Spect3D. The blue curve shows a Planck spectrum at the core temperature, and the green curve shows the emission spectrum as modeled by Eq. (18) with $A = 4.0 \times 10^{19}$ and the same core temperature.

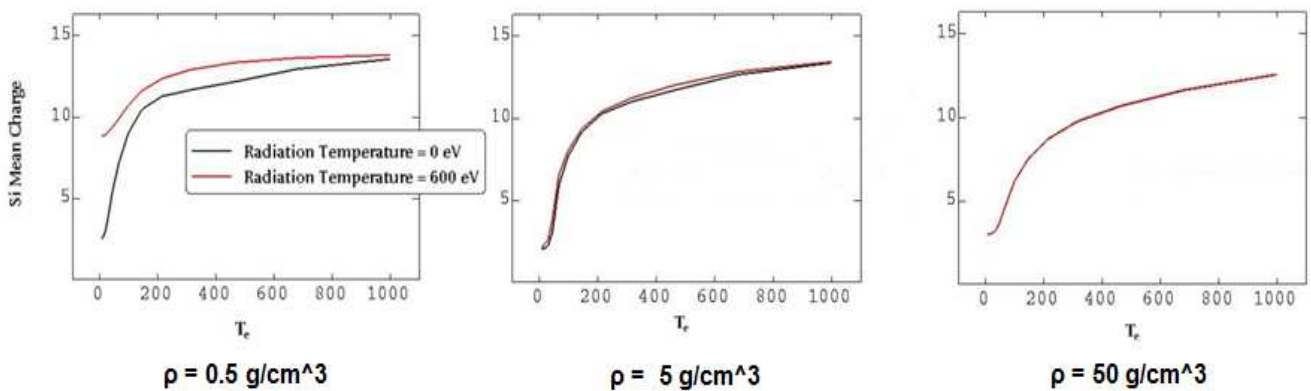


Figure 7: Mean charge of Si plasma dopant as a function of electron temperature T_e for three values of mass density ρ , with and without core radiation, as modeled by Eq. (17) with $T_S = 330 \text{ eV}$ and $T_R = 600 \text{ eV}$. The mean Si charge is strongly affected only at the lowest density.